

**This is an electronic reprint of the original article.**

**This reprint *may differ* from the original in pagination and typographic detail.**

**Author(s):** Thao Minh Ho, Felix Abik, Sami Hietala, Estefania Isaza Ferro, Leena Pitkänen, Dennis W. Juhl, Thomas Vosegaard, Petri O. Kilpeläinen & Kirsi S. Mikkonen

**Title:** Wood lignocellulosic stabilizers: effect of their characteristics on stability and rheological properties of emulsions

**Year:** 2022

**Version:** Published version

**Copyright:** The Author(s) 2022

**Rights:** CC BY 4.0

**Rights url:** <http://creativecommons.org/licenses/by/4.0/>

**Please cite the original version:**

Ho, T.M., Abik, F., Hietala, S. et al. Wood lignocellulosic stabilizers: effect of their characteristics on stability and rheological properties of emulsions. *Cellulose* (2022).

<https://doi.org/10.1007/s10570-022-04958-z>

All material supplied via *Jukuri* is protected by copyright and other intellectual property rights. Duplication or sale, in electronic or print form, of any part of the repository collections is prohibited. Making electronic or print copies of the material is permitted only for your own personal use or for educational purposes. For other purposes, this article may be used in accordance with the publisher's terms. There may be differences between this version and the publisher's version. You are advised to cite the publisher's version.



# Wood lignocellulosic stabilizers: effect of their characteristics on stability and rheological properties of emulsions

Thao Minh Ho · Felix Abik · Sami Hietala · Estefania Isaza Ferro · Leena Pitkänen · Dennis W. Juhl · Thomas Vosegaard · Petri O. Kilpeläinen · Kirsi S. Mikkonen

Received: 23 May 2022 / Accepted: 16 November 2022  
© The Author(s) 2022

**Abstract** Lignocellulosic materials from the forest industry have shown potential to be used as sustainable hydrocolloids to stabilize emulsions for many applications in life science and chemical industries. However, the effect of wood species and recovery method on the product's properties and ability to stabilize emulsions of isolated lignocellulosic compounds is not well understood. Hemicelluloses, abundant lignocellulosic side stream, exhibit differences in their water solubility, anionic character, lignin content, and degree of acetylation. Here, we explored

stability and rheological properties of model emulsions (5% hexadecane and 1% stabilizer, w/w) stabilized by different grades of sprucewood galactoglucomannan (GGM) and birchwood glucuronoxylan (GX) hemicelluloses. The results were compared to known soluble, insoluble, charged, and non-charged cellulosic stabilizers, namely methyl cellulose (MC), carboxymethyl cellulose (CMC), anionic- and non-ionic-cellulose nanocrystals (aCNC and dCNC). The results showed that GX emulsions were highly stable compared to GGM emulsions, and that deacetylation and lignin removal markedly reduced emulsion stability of GGM. Carboxymethylation to increase anionic characters enhanced the emulsion stabilization capacity of GGM, but not that of GX. Investigating flow behaviors of emulsions indicated that hemicelluloses primarily stabilize emulsions by adsorption of

---

Thao Minh Ho and Felix Abik contributed equally to this work.

---

**Supplementary Information** The online version contains supplementary material available at <https://doi.org/10.1007/s10570-022-04958-z>.

---

T. M. Ho (✉) · F. Abik (✉) · K. S. Mikkonen  
Department of Food and Nutrition, University of Helsinki,  
P.O. Box 66, FI-00014 Helsinki, Finland  
e-mail: minh.ho@helsinki.fi

F. Abik  
e-mail: felix.abik@helsinki.fi

T. M. Ho · K. S. Mikkonen  
Helsinki Institute of Sustainability Science (HELSUS),  
University of Helsinki, P.O. Box 65, FI-00014 Helsinki,  
Finland

S. Hietala  
Department of Chemistry, University of Helsinki, P. O.  
Box 55, FI-00014 Helsinki, Finland

E. Isaza Ferro · L. Pitkänen  
Department of Bioproducts and Biosystems, Aalto  
University, P.O. Box 16300, FI-00076 Aalto, Finland

D. W. Juhl · T. Vosegaard  
Danish Center for Ultrahigh-Field NMR Spectroscopy,  
Interdisciplinary Nanoscience Center and Department  
of Chemistry, Aarhus University, Gustav Wieds Vej 14,  
8000 Aarhus C, Denmark

P. O. Kilpeläinen  
Biorefinery and Bioproducts, Production Systems Unit -  
Natural Resources Institute Finland (Luke), Viikinkaari 9,  
FI-00790 Helsinki, Finland

insoluble particles, as their flow behaviors were similar to those of cellulose nanocrystals rather than those of soluble celluloses. Understanding the impact of the variations in composition and properties of hemicellulose stabilizers to stabilize emulsions allows tailoring of their recovery processes to obtain desirable hydrocolloids for different applications.

**Keywords** Spruce galactoglucomannan · Birch glucuronoxytan · Hemicellulose · Cellulose · Lignin

## Introduction

During the processing of emulsions, the addition of suitable stabilizers is required to achieve long-term stability. The added stabilizers will either adsorb onto the dispersed droplet surface to reduce interfacial tension or form a protective layer to prevent droplet aggregation, and/or increase the viscosity of the continuous phase to retard the movement of dispersed droplets (McClements 2005). As global consumers are now more conscious than ever about health and environment, their demand for innovative, cost-effective and clean-label stabilizers has increased significantly. Plant-based emulsifiers, especially those derived from wood, have emerged as great alternatives to replace their conventional counterparts. In addition to their natural, non-toxic, biodegradable, renewable nature, cost-effective, and versatile and abundant sources; wood-based stabilizers could possibly bring additional health benefits to produced emulsions due to their dietary fiber sources (Mikkonen 2020; Kynkäänniemi et al. 2022).

Wood biomass constitutes of 40–50% cellulose, 25–35% hemicelluloses, and 18–35% lignin (Sixta 2006). For the last two centuries, cellulose has been the main refining target, resulting in products such as fibers, nanocrystals and derivatives (Klemm et al. 2005). Many forms of cellulose, including derivatives and native forms, have been industrially produced as hydrocolloids, for example methyl celluloses, carboxymethyl celluloses, cellulose nanocrystals, ethyl hydroxyethyl cellulose and methyl ethyl hydroxyethyl cellulose (Heinze et al. 2018). All these different morphological and structural forms of cellulose have shown an amphiphilic character capable of acting as polymeric emulsifiers and Pickering stabilizers (Costa et al. 2021). Meanwhile, hemicelluloses are

treated as low-value by-products remaining outside of the biorefinery process. During cellulose refining, hemicelluloses, along with lignin, typically end up in water waste streams and are solely utilized to produce heat and energy (Mikkonen 2020). Therefore, to improve the sustainability of wood bioeconomy, biorefineries are expected to find efficient utilization and conversion methods for the valorization of all lignocellulosic components.

The most abundant hemicelluloses in softwoods (such as spruce) are galactoglucomannans (GGM), which comprise about 20% of wood mass. Regarding molecular structure, GGM has a linear backbone consisting of alternating  $\beta$ -(1 $\rightarrow$ 4)-D-glucopyranosyl (Glc $p$ ) and  $\beta$ -(1 $\rightarrow$ 4)-D-mannopyranosyl (Man $p$ ) units, and  $\alpha$ -(1 $\rightarrow$ 6)-D-galactopyranosyl (Gal $p$ ) side groups linked to the backbone Man $p$  units. Man $p$  units are partially acetylated at C-2 and C-3 positions with a degree of acetylation of 0.28–0.37 (Willför et al. 2008). On the other hand, hardwoods (such as birch) are rich in glucuronoxytans (GX), which account for about 25% of wood mass. GX has a linear backbone consisting of  $\beta$ -(1 $\rightarrow$ 4)-D-xylopyranosyl (Xyl $p$ ) units, and branched with (1 $\rightarrow$ 2)-linked 4-O-methyl- $\alpha$ -D-glucopyranosyl uronic acid (MeGlc $p$ A) and *O*-acetyl side groups (Sjöström 1993). Hemicelluloses have been efficiently recovered from the process water and spent sulfite liquor of thermo-mechanical pulping (TMP) (Al-Rudainy et al. 2018; Andersson et al. 2007), and from sawdust and wood chips using pressurized hot water extraction (PHWE) (Kilpeläinen et al. 2014), heat fractionation (Lundqvist et al. 2003), steam explosion (Chadni et al. 2019a), and high voltage electrical discharge (Chadni et al. 2019b). Depending on wood sources, recovery techniques, and their processing parameters, extracted hemicelluloses are markedly different in their chemical compositions and structural properties, consequently their ultimate functionalities and applications. Lignin and other wood-derived extractives are often co-extracted during the isolation of hemicelluloses, and the amounts of these residual materials typically increase with the increase of extraction temperature and time (Giummarella and Lawoko 2017). Extraction of GGM from spruce wood by PHWE at higher temperatures and for a longer time was reported to cause a lower pH level due to the release of uronic

acids from pectins and xylans, increasing the deacetylation and hydrolytic cleavage of GGM. As a result, the obtained GGM had less acetyl groups in its structure and a lower molar mass (Song et al. 2008; Juha et al 2012; Waqar et al. 2018). GGM extracted from thermomechanical pulping of spruce process water had a molar mass of 48,000 g/mol, being much higher than that obtained from PHWE (8200 g/mol) (Mikkonen et al. 2019). Hemicelluloses are partially water-soluble and exhibit both dissolved and aggregated morphologies (Bhattarai et al. 2020a, b). Degree of acetylation greatly affects the water solubility of hemicelluloses. It was reported that hemicelluloses with a high degree of acetylation are soluble only in aprotic solvents while non-acetylated hemicelluloses are partially soluble in hot water (Gröndahl et al. 2003). Extracted hemicelluloses can be further purified by ethanol precipitation to largely remove lignin (Willför et al. 2008), and chemically modified via carboxymethylation to enhance anionic character of hemicelluloses (Xu et al. 2011), to broaden the applications of hemicelluloses.

The utilization of GGM and GX in both native and derived forms as emulsion stabilizers have been well investigated (Bhattarai et al. 2019; Hannuksela and Holmbom 2004; Hromádková et al. 2005; Mikkonen et al. 2019, 2016a, 2009, 2016b; Xu et al. 2011). In previous studies, both GGM and GX were reported to have a good capacity to stabilize emulsions, and residual lignin and derivatization by carboxymethylation brought additional functionality. However, a systematic study is lacking to comprehensively compare the ability of these hemicelluloses in emulsion stabilization. In the present study, we investigate effects of chemical compositions, especially lignin and acetyl content, of five types of spruce galactoglucomannans (GGM) and three types of birch glucuronoxylans (GX), on stability and rheological properties of model emulsions (5% hexadecane and 1% stabilizer, w/w). A comparison of the emulsion properties between these hemicellulose stabilizers and established cellulosic stabilizers including both anionic and non-ionic soluble macromolecular stabilizers (methyl cellulose, MC and carboxymethyl cellulose, CMC) and Pickering stabilizers (anionic cellulose nanocrystal, aCNC and desulfated non-ionic cellulose nanocrystal, dCNC)

is also explored to reveal possible emulsion stabilization mechanisms of GGM and GX.

## Materials and methods

### Materials

The MC (Methocel™ A15LV) and CMC (Walocel™ CRT 30) were kindly gifted by Dupont (Meyrin, Switzerland). aCNC and dCNC were purchased from Cellulose Lab (Fredericton, Canada). High-acetyl (ha-) and low-acetyl (la-) GGM, and GX extracts recovered by PHWE (Kilpeläinen et al. 2014) were either spray-dried (ha-sGGM, la-sGGM and sGX), or ethanol-precipitated (la-eGGM and eGX), which were obtained from Natural Resources Institute Finland (Luke). High-acetyl ethanol precipitated GGM (ha-eGGM) was produced from ha-sGGM following the method reported by Bhattarai et al. (2019). The yield of spray-dried GGM (la-sGGM and ha-sGGM) and ethanol-precipitated GGM (eGGM) was 45–50% and 25–30% of original extract mass, respectively. Meanwhile, this value was 56–63% for spray-dried GX (sGX) and 24–28% for ethanol-precipitated GX (eGX).

The la-sGGM and eGX were carboxymethylated (CMGGM and CMGX) according to previously described methods (Petzold et al. 2006; Xu et al. 2011) with several modifications. 150 g hemicelluloses were dissolved overnight in 150–200 mL water. The slurry was then dispersed in 2.5 L of isopropanol at 65 °C, followed by the addition of 90 g NaOH (dissolved in 50 mL water). After one hour, 45 g of sodium monochloroacetate was added, and the mixture was left to react for 3 h under constant stirring. Once cooled down to room temperature, it was neutralized by dilute acetic acid, forming a dark liquid heavier than isopropanol. The product was decanted and dissolved in water, followed by antisolvent precipitation in methanol at 1:9 water:methanol (v/v). Following centrifugation (12000 g, 10 min) (Sorvall LYNX 6000, Thermo Scientific, Waltham, MA, USA), the residue was resuspended in methanol and centrifuged (12000 g, 10 min) twice. The final residue was then dispersed in methanol, filtered under vacuum, and dried overnight in a vacuum oven (Vacucenter 20, SalvisLab, Rotkreuz, Switzerland) at 40 °C. All samples are summarized in Table 1.

**Table 1** A summary of stabilizers utilized in this study

Stabilizer codes	Stabilizer names
ha-sGGM	High acetyl and spray-dried spruce galactoglucomannan
la-sGGM	Low acetyl and spray-dried spruce galactoglucomannan
ha-eGGM	High acetyl and ethanol-precipitated spruce galactoglucomannan
la-eGGM	Low acetyl and ethanol-precipitated spruce galactoglucomannan
CMGGM	Carboxymethylated spruce galactoglucomannan
sGX	Spray-dried birch glucuronoxylan
eGX	Ethanol-precipitated birch glucuronoxylan
CMGX	Carboxymethylated birch glucuronoxylan
MC	Methyl cellulose
CMC	Carboxymethyl cellulose
aCNC	Anionic cellulose nanocrystal
dCNC	Desulfated non-ionic cellulose nanocrystal

Hexadecane, sodium monochloroacetate, lithium bromide, trimethylchlorosilane (TMCS), bis(trimethylsilyl)trifluoroacetamide (BSTFA), acetyl chloride, acetyl bromide, acetic acid, perchloric acid, hydrochloric acid (HCl), *n*-heptane, isopropanol, pyridine, dimethyl sulfoxide (DMSO) and methanol were obtained from Sigma-Aldrich (St Louis, United States). Citric acid monohydrate was purchased from Merck (Darmstadt, Germany). Sodium hydroxide was obtained from Alfa Aesar (Massachusetts, United States). Softwood LignoBoost lignin was gifted by Stora Enso (Kotka, Finland). All chemicals used in this study were of analytical or synthesis grade.

### Characterization of stabilizers

#### *Carbohydrate analysis*

The carbohydrate composition of the hemicellulose samples was determined in triplicate by gas chromatography (GC) analysis of the silylated methanolysate (Chong et al. 2013; Laine et al. 2002; Sundberg et al. 1996). 10 mg of each hemicellulose sample were methanolized by 2 mL HCl 3 M in dry methanol for 3 h at 100 °C. Following neutralization by pyridine and dissolving in 10 mL methanol, 600 µL aliquots were silylated by TMCS:BSTFA 1:99 (v/v) at room temperature overnight. The silylated product was dissolved in 1 mL heptane and run through a GC (HP 6890 N, Agilent Technologies, Waldbronn, Germany) with a flame ionization detector, equipped with a DB-1 column (30 m, i.d. 0.25 mm, 0.25 µm film). 1 µL sample was injected and eluted at 20:1 split ratio

using the following temperature program: 150 °C (held for 3 min)—increasing at 2 °C/min to 186 °C—then 1 °C/min to 200 °C—and further 20 °C/min to 300 °C (held for 1 min). Sorbitol was used as an internal standard. Arabinose, rhamnose, xylose, glucose, galactose, and galacturonic acid were quantified by a standard curve constructed using the peak area of the highest peak of each corresponding sugar, while methyl glucuronic acid was approximated using the two main peaks of the sodium salt of glucuronic acid (Chong et al. 2013). The mass of the sugars was then corrected for water condensation (pentoses 0.88, hexoses 0.9, uronic acids 0.91).

#### *Lignin content*

The lignin content of the hemicellulose samples was determined by acetobromination (Carvalho et al. 2020) using a standard addition method. 20 mg of the hemicelluloses were mixed with 5 mL of 25% acetyl bromide in acetic acid glacial and 0.1 mL perchloric acid in a capped glass tube, mixed by vortexing. The mixture was heated for 30 min at 70 °C, gently shaking the tube at 10-min intervals. Afterwards, the mixture was cooled in an ethanol-ice bath for 10 min, then 5 mL of ice cold NaOH 2 M was added, letting it cool down for another 10 min. The mixture was then transferred to a 25-mL volumetric flask and topped up with acetic acid glacial. A stock standard lignin solution (using softwood LignoBoost lignin) and a blank solution were prepared at the same time. 1-mL aliquots of sample solution were added to 4 10-mL volumetric flasks, spiked with an increasing amount

of lignin. The series were then analyzed by measuring absorbance (Shimadzu UV-1800, Shimadzu Corp., Kyoto, Japan) at 280 nm, plotting the amount of added lignin against measured absorbance, and extrapolating the plot to obtain the amount of lignin. Each hemicellulose was analyzed in duplicate.

### Molar mass analysis

Molar mass values of the hemicelluloses were estimated by DMSO-based and water-based size-exclusion chromatography (SEC), except for CMGX and CMGGM which were insoluble in DMSO. DMSO-SEC was performed on GPCMax (Viscotek Corp, Houston, TX, USA) equipped with Jordi xStream GPC column (Jordi Labs, Mansfield, MA, USA) at 60 °C with 0.01 M LiBr in DMSO as the eluent at 0.8 mL/min flow rate; recorded data were processed using OmniSEC 4.6 software. Water-SEC was performed on Agilent 1260 Infinity II Multi-Detector GPC/SEC System (Agilent Technologies, Santa Clara, CA, USA) equipped with three Waters 7.8 mm×300 mm Ultrahydrogel columns (500, 250, and 120 Å) and a 6 mm×40 mm Ultrahydrogel guard column, using 0.1 M NaNO<sub>3</sub> in demineralized water as the eluent at 0.5 mL/min; recorded data were processed using Agilent GPC/SEC software. 2 mg/mL hemicelluloses were dissolved in the eluent and filtered through a 0.45 µm syringe filter (Acrodisc 13 mm minispikes wvPTFE, Pall Corp, Ann Arbor, MI, USA). 100 µL of the resulting solutions were injected and eluted isocratically through the respective SEC system. Eluted peaks were detected by refractive index (RI, at 40 °C), ultraviolet (UV, 280 nm), as well as low- and right-angle light scattering (LALS (7°) and RALS (90°), 670 nm) detectors. Weight-average (M<sub>w</sub>) and number-average (M<sub>n</sub>) molar mass values were estimated using pullulan calibration curve from the RI signal. We used pullulan with nominal peak apex molar mass (M<sub>p</sub>) of 342, 5900, 11,800, 22,800, and 113,000 g/mol for the DMSO-system and 342, 1080, 6100, 9600, and 21,100 g/mol for the water-system.

### Degree of acetylation

The acetyl contents of the hemicelluloses are presented as degree of acetylation, which was determined in duplicates only for non-derivatized samples,

as the carboxymethylation procedure used a strongly-alkali condition which completely removed all the acetyl groups (Xu et al. 2011). The absence of acetylation in the CMGX and CMGGM samples were also confirmed by the nuclear magnetic resonance (NMR) and Fourier-transform infrared (FTIR) spectra (Figures S1 and S2, respectively), and therefore we did not determine their degrees of acetylation. Approximately 100 mg of each hemicellulose sample was dissolved in 10 mL NaOH 0.1 M and incubated overnight under stirring. The dispersions were then neutralized to pH 6.5–7.5 by HCl 0.83 M, followed by dilution to 25 mL with milliQ water. After a gentle shaking, 1 mL aliquot was centrifuged at 15,000 rpm for 20 min. 50 µL of the supernatant was subsequently analyzed by the Acetic Acid Kit (K-ACET, Megazyme, Ireland). As all the samples contain lignin that also absorbs light at 340 nm, separate blanks were made for each hemicellulose by substituting the final 20 µL of acetyl CoA synthase with water. The acetyl content was calculated as moles of acetyl per 100 g of anhydrous backbone polysaccharide using the molecular weight of acetyl group (43 g/mol) and adjusting the calculated values by the mass percentage of backbone monosaccharides (mannose and galactose for GGMs, xylose for GX). The degree of acetylation ( $D_A$ ) was then calculated using the following equation (Eq. 1) (Xu et al. 2010):

$$D_A = \frac{M_s \times \%_{\text{acetyl}}}{(M_{\text{acetyl}} \times 100) - (M_{\text{acetyl}} - 1) \times \%_{\text{acetyl}}} \quad (1)$$

Where  $M_s$  is the molar mass of anhydrate sugar unit (162 for hexoses, 132 for pentoses),  $M_{\text{acetyl}}$  is the molar mass of acetyl unit (CH<sub>3</sub>CO), and  $\%_{\text{acetyl}}$  is the acetyl content.

### Additional characterization of carboxymethylated hemicelluloses

Complete deacetylation and carboxymethylation were demonstrated qualitatively by a Fourier transform infrared spectrometer (PerkinElmer, Waltham, MA, USA). The background of clean zinc selenide crystal was obtained before scanning for the samples. The samples were placed on the crystal and compressed by ART arm with a fixed degree of compression at 80%. The scanning frequencies ranged from 4000 to

650  $\text{cm}^{-1}$ . Spectra resolution was 4  $\text{cm}^{-1}$ , and the number of scans were 16.

The degree of carboxymethylation for CMGX and CMGGM was determined by quantitative solid-state NMR under the assumption that the lignin moieties were not affected by the carboxymethylation process. Quantitative  $^1\text{H}$ - $^{13}\text{C}$  NMR experiments were obtained by multiple cross-polarization blocks (MultiCP) (Johnson and Schmidt-Rohr 2014) and were performed on a Bruker 700 MHz NMR spectrometer (Bruker Biospin, Rheinstetten, Germany) using a 4-mm  $^1\text{H}$ -X-Y broadband magic-angle spinning probe configured in double-resonance mode and employing a 9.5 kHz spin rate. The measurements used 10 cross-polarization steps of 1 ms each (at RF field strength of ca. 69 and 41 kHz for  $^1\text{H}$  and  $^{13}\text{C}$ , respectively) with a 1.5 s delay between the steps,  $^{13}\text{C}$  signal acquisition under SPINAL-64 1H decoupling with an RF field strength 94 kHz, and 2.5 s recycling delay. The acquired spectra were processed using Bruker TopSpin 4.0.7 with a line broadening of 10 Hz, and referenced externally using adamantane (38.48 ppm). The degree of carboxymethylation ( $D_{\text{CM}}$ ) was calculated by comparing the integration of carboxyl signal of the carboxymethyl moiety in the range of 172 ppm to 186 ppm ( $I_{172-186 \text{ ppm}}$ ) to the anomeric C1 signal ( $I_{94-110 \text{ ppm}}$ ) (Eq. 2) based on the spectra of the carboxymethylated hemicelluloses (Xu et al. 2011):

$$D_{\text{CM}} = \frac{I_{172-186 \text{ ppm}}}{I_{94-110 \text{ ppm}}} \quad (2)$$

The presence of hexenuronic acid (HexA) in CMGX and CMGGM were analyzed using ultraviolet-resonance Raman (UVR) spectroscopy (Jääskeläinen et al. 2005). Powdered samples were pressed on a cellulose filter paper to form a flat substrate to be measured using Renishaw 1000 UV Raman spectrometer (Gloucestershire, UK) coupled with a Leica DMLM microscope (Wetzlar, Germany) and an Innova 300C FreD frequency-doubled Ar<sup>+</sup> ion laser (Coherent Inc., Santa Clara, CA, USA). UVR spectra were recorded using a 244 nm laser focused by a 50  $\mu\text{m}$  slit, with a spectral range of 640–1865  $\text{cm}^{-1}$  at approximately 3.7  $\text{cm}^{-1}$  resolution. The samples were rotated at 6 rpm to obtain an averaged spectrum and to avoid excessive

damage from laser exposure. For each sample, at least 3 spectra were collected. The recorded spectra were averaged and processed using Grams/32 software. The recorded spectra of the carboxymethylated hemicelluloses and their respective precursors are presented in Figure S3. As the hemicelluloses did not contain any trace of cellulose, and that the specific signals for xylans and mannans (Wang et al. 2020; Zeng et al. 2016) were not detected as viable peaks, we could not determine the amount of HexA quantitatively. We instead normalized the intensity of HexA band (1655  $\text{cm}^{-1}$ ) of CMGX and CMGGM to their respective lignin intensity (1605  $\text{cm}^{-1}$ ) and compared them with the lignin-normalized signals of their respective precursors eGX and la-eGGM, to obtain an estimated ratio of how much HexA was produced by the synthesis relative to lignin content.

#### Emulsion preparation

Hexadecane emulsions with different stabilizers were prepared by following the method reported by Valoppi et al. (2019) with a slight modification. All emulsions had 1% (w/w) stabilizer and 5% (w/w) hexadecane. The selected stabilizers were dispersed in a 25 mM citric buffer (pH=4.5) using a magnetic stirrer for at least 24 h to produce continuous phases. For aCNC and dCNC stabilizers, after being mixed with the buffer and stirred at least overnight, the mixtures were immersed in an ice bath and sonicated (Branson 450 Digital Sonifier, Marshall Scientific, Hampton, USA) at 50% amplitude using a 10 s on and 10 s off cycle for a total of 20 min (corresponding to 10 min of exposure) to enable the complete dispersion of the stabilizers. Hexadecane was then added to the continuous phase, and an Ultra-Turrax homogenizer (T-18 basic, IKA, Staufen, Germany) equipped with S25N-18G dispersing head at 8,000 rpm for 2 min was applied to obtain coarse emulsions while avoiding excessive foaming. The fine emulsions were achieved by using a high-pressure homogenizer configured with 75 mm Y-type F20Y and 200 mm Z-type H30Z chambers in a series (Microfluidizer 110Y, Microfluidics, Westwood, MA, USA) at 800 bar for three consecutive cycles. The emulsions were collected in 50 mL falcon tubes for further analysis.

## Emulsion characterization

The emulsions kept standing in the falcon tubes were stored at room temperature ( $\sim 22$  °C). The emulsion properties (except for Turbiscan which was measured at 0, 6, 24, 48 and 96 h) were characterized within 1 h after preparation ( $t=0$ ) and after 96 h. The 96 h storage period was selected as we avoided using any preservatives which might affect emulsion properties. For all measurements, except for Turbiscan, the samples were gently turned upside down 15 times before analysis.

### $\zeta$ -potential

The  $\zeta$ -potential of oil droplets in emulsions were measured using an electrophoretic light scattering instrument (Zetasizer Nano ZS series, Malvern Panalytical Ltd, Malvern, UK). The samples were diluted 1:2000 in a 25 mM citric buffer (pH=4.5) to avoid multiple scattering effects. The diluted samples were loaded in a disposable folded capillary cell (DTS1070, Malvern Panalytical Ltd, Malvern, UK) and inserted to the instrument. After equilibration at 22 °C for 1 min, three  $\zeta$ -potential readings for each measurement were obtained. At least two measurements for each sample were performed.

### Droplet size and its distribution

Oil droplet size and its distribution of emulsions were determined by using a laser light scattering analyzer (Mastersizer Hydro 3000 SM, Malvern Instruments Ltd, Malvern, UK) connected with a dispersion accessory (Hydro EV, Malvern Instruments Ltd, Malvern, UK), and water as dispersant. During measurement, the rotor speed was set at 1500 rpm, and reflective indices of water and hexadecane were 1.33 and 1.434, respectively. At least two measurements (with three readings for each measurement) for each sample were performed.

### Droplet morphology

The morphology of oil droplets in emulsions was visualized using an optical microscope (AxioVision, Carl Zeiss, Microimaging GmbH, Jena, Germany) equipped with a digital camera (AxioCam MRm, Carl Zeiss, Microimaging GmbH, Jena, Germany). A drop

of emulsion was placed in the middle of a glass slide and covered with a glass coverslip. The dispersed droplet morphology was observed under a 100X objective with a drop of mineral oil.

### Turbiscan

The physical stability of emulsions during storage at 22 °C over 96 h was determined by a Turbiscan Lab Expert analyzer (Formulations, France). Approximately 20 mL of freshly made emulsions were transferred to transparent glass vials and they were kept undisturbed during storage. The stability of emulsions is evaluated using the global Turbiscan stability index (TSI), which were subjected to non-linear regression analysis following Eq. (3) using TableCurve 2D software (Jandel Scientific, version 5.01) in which the Levenberg–Marquardt algorithm is applied to Least Squares minimization.

$$\text{TSI} = \text{TSI}_{\max} (1 - e^{-K \cdot t}) \quad (3)$$

where TSI is the Turbiscan stability index,  $\text{TSI}_{\max}$  is the maximum TSI reachable at infinite times,  $K$  is the rate constant, and  $t$  is time (h). The goodness of curve fitting was evaluated based on the residual analysis and fitting parameters ( $r^2$ ,  $p$ -value and standard error).

### Rheological properties

Rheological behaviors of continuous phases and emulsions were determined at 22 °C using DHR-2 rheometer (TA Instruments, New Castle, USA) with a double wall concentric cylinder geometry (inside and outside cup diameter of 40 and 44.58 mm, respectively; inside and outside bob diameter of 40.76 and 43.92 mm, respectively; and operating gap of 500  $\mu\text{m}$ ). About 7.5 mL of each sample was carefully injected into the measuring cup. After lowering the bob into the measuring cup, the bobs were slightly moved back and forth several times to remove any air bubbles in the sample cup, and then the samples were equilibrated for 5 min.

Flow sweep measurements were performed over a shear rate range of 0.1–100 and 0.1–1000 1/s with two cycles for each range: increasing of shear rate from 0.1 to 100 or 1000 1/s and decreasing of shear rate from 100 or 1000 1/s to 0.1 1/s. Differences in the viscosity between two cycles (also known as



hysteresis loop) indicate the structural changes of the samples due to shearing. Viscosities of plain citric buffer and hexadecane were also determined by flow sweep measurements with two cycles of shear rate in a range of 0.1–1000 1/s.

For emulsions, linear viscoelastic moduli (frequency oscillatory test) were measured at a strain amplitude of 1% and the angular frequencies from 600 to 0.01 rad/s; and large amplitude oscillatory shear flow measurements were carried out at strain amplitudes from 0.01 to 700% at the angular frequencies of 1 and 20 rad/s.

## Results and discussion

### Characterization of stabilizers

Carbohydrate analysis (Table 1) showed several variations in the proportion of individual monosaccharides compared to previously reported values

(Mikkonen et al. 2019; Valoppi et al. 2019), but in general the main constituents were still GGM and GX in the respective materials. One noticeable difference between the ha-GGM and la-GGM (for both spray-dried and ethanol-precipitated) is that while both show the presence of normally-occurring arabinoxylan (Schönberg et al. 2001) the la-GGM has a higher proportion of xylose, indicating a higher proportion of arabinoxylan. Presence of galacturonic acid (GalA) indicates traces of pectin (Sundberg et al. 1996), which in the case of GX was eliminated by ethanol precipitation; in the case of la-GGM, they are still present in a small amount. For the carboxymethylated samples, the proportion of all carbohydrates were reduced compared to their precursors, indicating that the carboxymethylation did not target any specific sugar. However, some individual sugars decreased more than the others, which might have been related to their relative availability towards carboxymethylation in isopropanol.

**Table 2** Analyzed characteristics of GGM and GX stabilizers

Properties	Stabilizers (*)							
	ha-eGGM	ha-sGGM	la-eGGM	la-sGGM	CMGGM	sGX	eGX	CMGX
Lignin content (g/100 g)	7.26±0.07	17.20±0.47	9.04±1.67	16.11±0.56	8.68±0.11	24.63±3.82	15.26±0.07	18.67±0.01
Degree of acetylation (-)	0.34	0.33	0.13	0.21	n.d	0.77	0.62	n.d
Degree of carboxymethylation (-)	n.d	n.d	n.d	n.d	0.46	n.d	n.d	0.33
Molar mass ( <i>M<sub>w</sub></i> , g/mol)/Dispersity (-)								
DMSO	3100/2.4	4100/4.1	5400/3.6	4100/6.1	n.d	2800/4.8	3500/2.0	n.d
Water	2800/1.7	2800/1.7	7500/2.2	8300/2.9	13,000/4.0	3600/2.5	3600/1.8	7600/1.7
Carbohydrate composition (g/100 g)								
Arabinose	n.d	n.d	n.d	1.17±0.18	n.d	n.d	n.d	n.d
Rhamnose	n.d	0.63±0.63	n.d	n.d	n.d	0.91±0.04	0.8±0.05	0.67±0.03
Xylose	6.18±0.38	6.53±0.33	9.61±0.47	10.15±1.09	4.65±2.06	53.21±0.71	55.36±3.07	35.02±1.76
Galactose	7.11±0.28	6.71±0.45	6.92±0.24	6.84±0.76	3.37±1.19	1.56±0.04	2.30±0.19	0.10±0.01
Mannose	44.09±2.40	43.37±2.55	37.72±1.56	36.27±4.12	24.61±1.49	2.50±0.11	3.63±0.19	2.40±0.09
Glucose	11.75±0.60	11.28±0.71	9.64±0.39	9.19±1.05	6.63±0.35	1.92±0.09	5.06±0.25	3.49±0.20
Galacturonic acid	n.d	n.d	2.48±0.11	2.19±0.25	n.d	1.98±0.09	n.d	n.d
Methyl glucuronic acid	n.d	n.d	n.d	n.d	n.d	7.33±0.22	7.11±1.01	7.08±0.23

(\*) Please refer to Table 1 for the sample codes. n.d. = Not determined, DMSO = Dimethyl sulfoxide solution

As shown in Table 2, the spray-dried hemicelluloses have higher amounts of lignin compared to the ethanol-precipitated ones. However, it appears to be counterintuitive that CMGX has a higher lignin content than eGX, as the synthesis process did not involve the addition of lignin. We therefore performed UVRR spectrometry to determine the presence of hexenuronic acid (HexA). HexA is known to be formed during alkaline pulping by the degradation of uronic acid residues within the hemicelluloses (Teleman et al. 1995). As the synthesis of the carboxymethylated derivatives involve highly alkaline condition and an elevated temperature, combined with the fact that GX has a significant amount of glucuronic acid residues, it is justified to suspect that the interference might have come from HexA. The UVRR result confirmed the presence of HexA, which absorbs UV light at 280 nm, giving an overestimation of the lignin content for both the derivatives and their respective precursors. We also detected HexA in the precursor GX; unfortunately, it was not possible to quantify the amount of HexA properly, as the quantitative aspect of the UVRR-based method relied on the presence of a standard cellulose peak to normalize the HexA signal, or a standard xylan and mannan peak, which were not detected. Therefore, we normalized the HexA signals of CMGX and its precursor eGX to their respective lignin signals, and then presented the result as a ratio of the lignin-normalized HexA intensity between the derivatized product and the precursor. The obtained lignin-normalized HexA ratio between the product and the precursor of 2.36 for CMGX indicates that, assuming the lignin content did not change, there had been a two-fold increase in the amount of HexA, which led to the overestimation of the lignin content in CMGX. A similar increase of HexA content leading to lignin overestimation also happened for CMGGM, although the extent is not as severe as CMGX, with a ratio of 1.39. The source of glucuronic acid residues that gave rise to HexA in CMGGM might have been the trace xylans, whose amount of glucuronic acid is sufficiently low to not be detected by the carbohydrate analysis method, but once converted into HexA is enough to cause some interference. Nevertheless, we believe that in reality the amount of lignin in CMGX and CMGGM would have been less than their precursors, as the lignin could have been partially dissolved in the methanol

(Melro et al. 2018) used as the antisolvent to separate the products.

In general, GX has higher DA values compared to GGM. Additionally, the four types of GGM we used in this study can be divided into low-acetyl (la-) and high-acetyl (ha-) GGM, where we observed that their solubility and emulsion stabilizing capabilities differ (details can be found in the section of emulsion properties). The absence of acetyl groups in CMGX and CMGGM was indicated by the absence of carboxyl resonances around 175 ppm on the  $^{13}\text{C}$  solid-state NMR spectra of CMGX and CMGGM (Figure S1 in the supplementary materials). This carboxyl resonance from the acetyl group was visible in the spectrum for eGX and appeared weakly in la-eGGM, and was replaced by the carboxyl resonance from carboxymethyl moiety around 178 ppm. We also performed additional confirmation by FTIR (Figure S2), where the absorption at  $1730\text{ cm}^{-1}$  (corresponding to C=O ester carbonyl stretch of the acetyl groups) diminished from the CMGX and CMGGM spectra while being replaced by sharp absorption at  $1600\text{ cm}^{-1}$  (corresponding to C=O carboxyl stretch of the carboxymethyl groups) (Candido and Gonçalves 2016).

In general, as indicated in Table 2, the molar mass values obtained from DMSO SEC appear to be smaller than in water, which might mean that the hemicellulose chains are folded more compactly in DMSO, corresponding to a smaller molar mass value. However, an opposite trend is observed for GGM with higher degrees of acetylation (ha-sGGM and ha-eGGM), where they have a lower molar mass in water compared to DMSO. Additionally, all hemicelluloses have high molar mass dispersity. One interesting aspect to point out is how CMGGM and CMGX have about twice the molar mass of their respective precursors la-eGGM and eGX. The addition of carboxymethyl moieties in the hemicellulose chains might have caused conformational changes which influenced the measured molar mass. Moreover, the requirement to filter the samples prior to injection into the SEC system might have eliminated any aggregates or larger structures that formed prior to filtering, which could play an important role in the emulsion stabilization. With all these observations, the molar mass values must be interpreted cautiously, and it is difficult to correlate any observable phenomenon to the molar mass of the hemicelluloses.

## Properties of emulsions

 $\zeta$ -potential

The  $\zeta$ -potential values of oil droplets in emulsions express the magnitude of their surface charge, and thus the degree of electrostatic repulsion which prevents the oil droplets from coalescence and aggregation. The higher absolute  $\zeta$ -potential values impart a higher electrostatic repulsion between adjacent oil droplets, and result in a higher stability of emulsions (McClements 2005). Generally, an emulsion is highly stable only as its  $\zeta$ -potential value higher than 30 mV (Bhattacharjee 2016). As indicated in Fig. 1, all emulsions had a negatively charged surface. Oil droplets stabilized by GGM (1a-sGGM, 1a-eGGM, ha-sGGM and ha-eGGM) had very low absolute  $\zeta$ -potential values (3.22–8.52 mV), and as expected this low electrostatic repulsion did not contribute to emulsion stabilization. The  $\zeta$ -potential values of GGM samples determined in this study are highly compatible to those reported in previous studies (Mikkonen et al. 2016b; Valoppi et al. 2019).

GX emulsions (eGX and sGX) had higher absolute  $\zeta$ -potential values (12.15–13.53 mV) than GGM counterparts, which is possibly because a higher content of the anionic methyl glucuronic acid and galacturonic acid residues was found in GX (Table 2). The

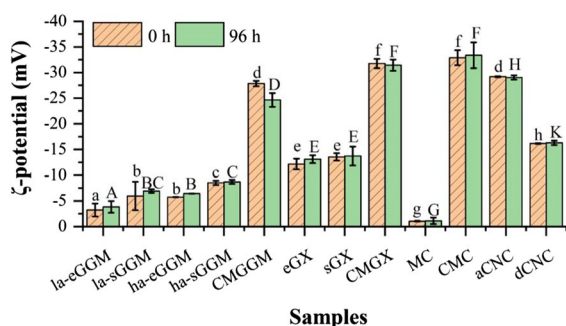


**Fig. 1**  $\zeta$ -potential values of oil droplets in emulsions prepared from different stabilizers as fresh ( $t=0$ ), and after 96 h of preparation. Please refer to Table 1 for the sample codes. A one-way analysis of variance (ANOVA) and Tukey test were used as a post-hoc test for a pairwise comparison of the means with a statistically significant difference at  $p \leq 0.05$  using OriginPro 2020 (OriginLab Corporation, Northampton, MA, USA). Within the same time point (either 0 or 96 h), means with different letters indicated statistically significant differences among samples

presence of these anionic surface charge residues could impart a higher emulsion stabilization capacity to GX than GGM. However, for either GGM or GX, differences in lignin content and sugar composition did not have a major effect on  $\zeta$ -potential values of their emulsions. Similar results were also found for GGM samples at different degrees of acetylation.

The introduction of negatively charged carboxymethylated groups made the surface charge of oil droplets in CMGGM and CMGX emulsions to be more negative, with a higher degree of a negatively charge increase being observed for CMGX due to the presence of anionic methyl glucuronic acid (Table 2). Due to similarity in  $\zeta$ -potential values of CMGGM, CMGX, CMC and aCNC, it is expected that the carboxymethylation of hemicelluloses could increase their ability to stabilize emulsion. Difference in absolute  $\zeta$ -potential between aCNC (29.18 mV) and dCNC (16.15 mV) can be explained by their sulfate content, by which aCNC with the higher amount of sulfate content had the higher negative surface charge (Pandey et al. 2018).

During 96-h storage, all samples, except for CMGGM emulsion displaying the slight reduction of absolute  $\zeta$ -potential, maintained their  $\zeta$ -potential values unchanged. The changes in surface charge of CMGGM emulsion during storage were possibly caused by desorption of CMGGM stabilizer from the oil droplet interface and/or charge neutralization effect, which require further investigation to provide a concrete conclusion.

## Droplet size and its distribution

The size of oil droplets in emulsions were measured as fresh ( $t=0$  h), and at 6 and 96 h after preparation to evaluate their stability. The average size of oil droplets in terms of  $D[3,2]$ ,  $D[4,3]$ ,  $Dv(10)$ ,  $Dv(50)$  and  $Dv(90)$  can be found in Table S1 (Supplementary materials), and here we reported the size distribution of oil droplets (Fig. 2).

For freshly prepared emulsions ( $t=0$ ), all GGM and GX samples exhibited bi- or tri-modal droplet size distribution (DSD) with one or two peaks larger than  $0.5 \mu\text{m}$  representing droplet diameter. However, unlike the DSD of GGM-stabilized emulsions which included two distinguished peaks representing droplets smaller and larger than approximately  $1.0 \mu\text{m}$  (Fig. 2a–e), those of GX-stabilized emulsions

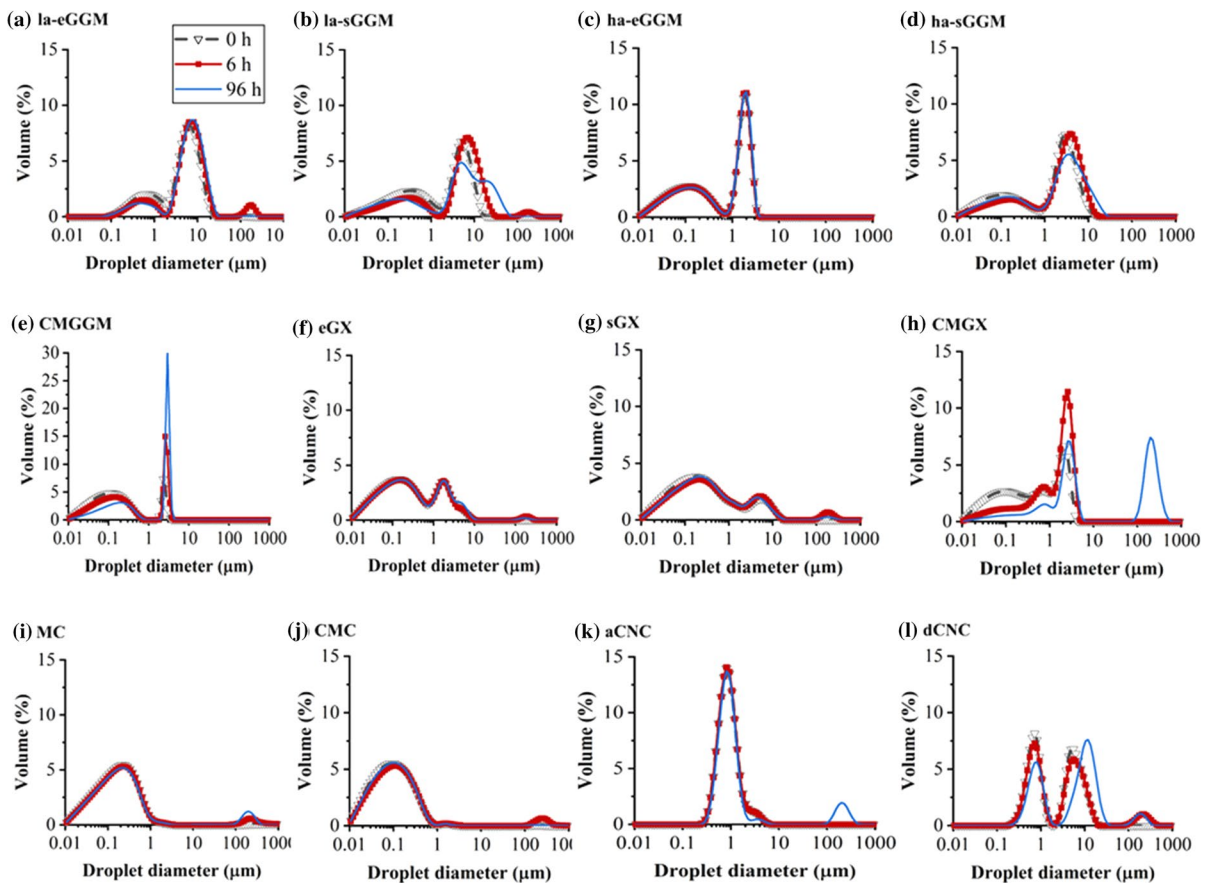


**Fig. 2** Size distribution of oil droplets in emulsions stabilized by different emulsifiers as fresh ( $t=0$ , black dotted lines with triangle symbols), and after 6 (red solid lines with square sym-

bols) and 96 h (blue solid lines) of preparation. Please refer to Table 1 for the sample codes

exhibited a main peak at around  $0.1 \mu\text{m}$  and a shoulder at a higher droplet size (Fig. 2f–h). Although the similar DSD patterns were observed for all GGM emulsions, the intensity and width of these peaks were markedly different, which indicates effects of their characteristics regarding lignin content, degree of acetylation, molar mass, carbohydrate composition, and surface charge on the resultant emulsion droplet size. Similar results were also witnessed for all GX emulsions. In previous studies (Bhattarai et al. 2019; Lahtinen et al. 2019; Valoppi et al. 2019), differences in DSD of emulsions prepared from GGM and GX at different lignin content were also reported despite the difference in oil phase used in these studies (e.g., rapeseed oil). For cellulose-stabilized emulsions, MC and CMC had almost identical mono-modal DSD curves with a droplet diameter of

$0.01\text{--}1.0 \mu\text{m}$ , and similar to aCNC emulsions but with a larger droplet diameter range ( $\sim 0.5\text{--}5 \mu\text{m}$ ) while dCNC had bi-modal DSD with two peaks ( $0.5\text{--}3 \mu\text{m}$  and  $0.5\text{--}13 \mu\text{m}$ ) almost equal in volume percentage.

Evaluating both  $D[4,3]$  and  $D[3,2]$  values (Table S1) of freshly prepared hemicellulose-stabilized emulsions revealed that GGM produced emulsions with much larger oil droplet diameters than GX. For GGM stabilizers, removing acetyl groups and/or lignin increased the oil droplet diameter while introducing negatively charge led to an opposite effect on the oil droplet diameter. Similar effects of removing lignin and introducing negative charge on oil droplet diameter were also found for GX stabilizers. The oil droplet diameter of emulsions was reported to be highly dependent on the types of stabilizers used due to their differences in the rate of diffusion and

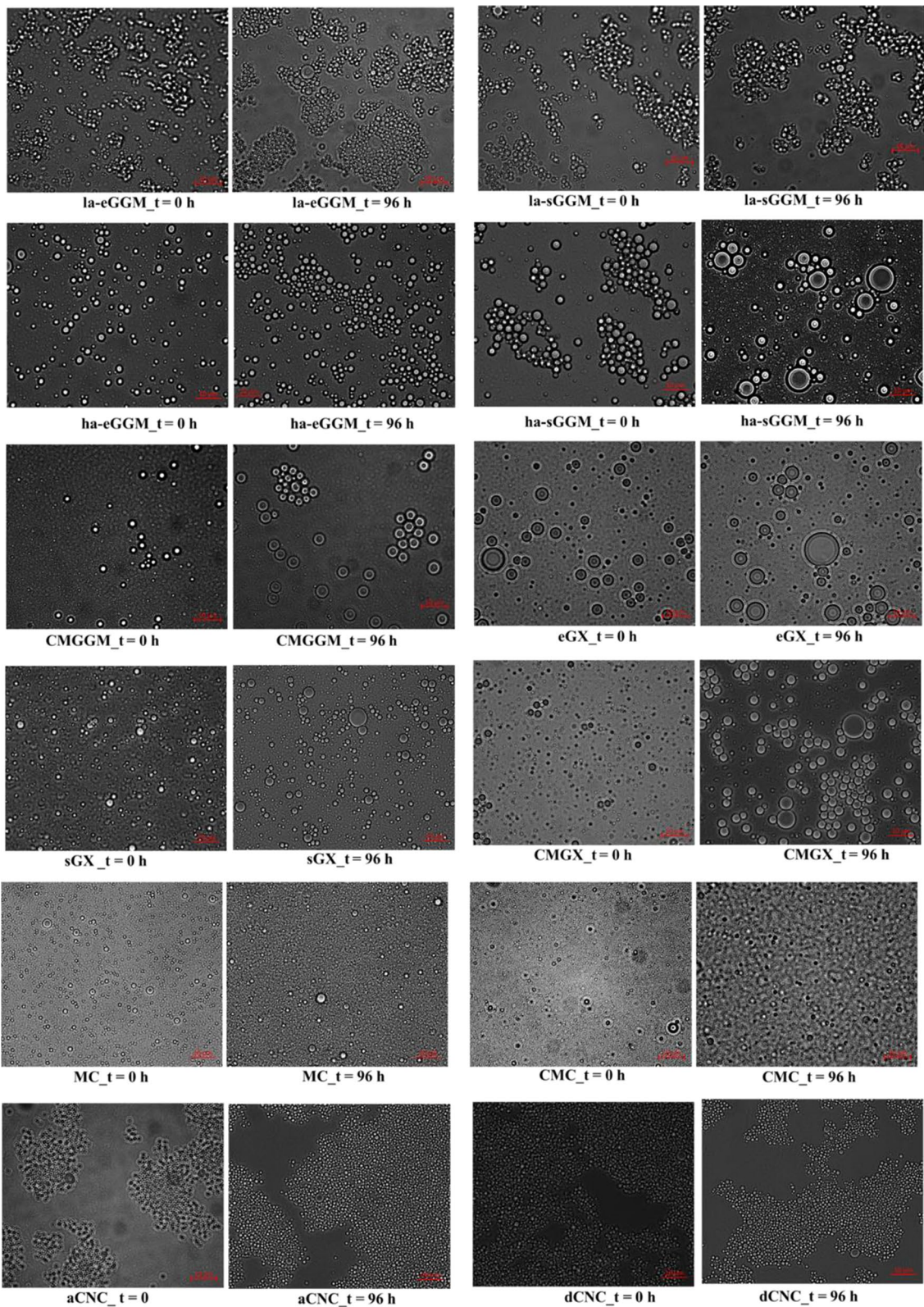


**Fig. 3** Optical microscopic images of oil droplets in emulsions prepared from different stabilizers as fresh ( $t=0$ ) and after 96 h of storage. Scale bar = 10  $\mu\text{m}$ . Please refer to Table 1 for the sample codes

adsorption onto interfacial regions formed during emulsification. The stabilizers with the higher diffusion and adsorption rate allow more rapid formation of submicron emulsion droplets (O'sullivan et al. 2015). Stabilizers with a lower molar mass have a higher diffusion and adsorption rate, and therefore capable to produce smaller emulsion droplet size (Tadros 2016). However, this concept is not supported by the analytical results about molar mass of GGM and GX stabilizers (Table 2) as no clear correlation was observed between their molar mass and their respective emulsion oil droplet diameter. For examples, among hemicellulose stabilizers, CMGGM had the highest molar mass (e.g., 13,000 g/mol) but its emulsion had the smallest oil droplet diameter ( $D[3,2] \approx 0.07 \mu\text{m}$ ) while la-eGGM had a molar mass of 7500 g/mol and its oil droplets had the highest  $D[3,2]$  value (1.40  $\mu\text{m}$ ). Therefore, other factors, such as viscosity of continuous phase, molecular structure, and solubility of stabilizers might be more important to their diffusion and adsorption rate than molar mass. Soluble celluloses such as MC and CMC were able to produce emulsions with very small oil droplets ( $D[3,2] \approx 0.06\text{--}0.09 \mu\text{m}$ ) while cellulose nanocrystals (aCNC and dCNC) produced much larger oil droplets ( $D[3,2] \approx 0.81\text{--}1.14 \mu\text{m}$ ). The large size of oil droplets in CNC emulsions could be explained by their rod-like and rigid structure, which could interfere the droplet formation during emulsification and some oil droplets coalesce before the oil droplets are fully covered by CNC (Bai et al. 2019).

Over the 96 h of storage, the changes in DSD were observed for all studied emulsions with the most significant alteration being observed for CMGGM, CMGX, aCNC, and dCNC samples. In their DSD, there was a marked increase in volume percentage of large droplet size and/or appearance of a new peak for droplet diameter around several hundreds of micrometres. In addition, the average droplet diameters,  $D[4,3]$  and  $D[3,2]$  of all studied emulsions increased even after 6 h of preparation (Table S1). Visual observation of studied emulsions revealed that all GGM- and GX-stabilized emulsions were creaming after 96 h of storage, but after gentle shaking, the creaming

layers were redispersed, and their droplet size recovered to almost the original values. Meanwhile, the cellulose-stabilized samples (MC, CMC, aCNC and dCNC emulsions) did not have any visual signal of creaming, suggesting that increasing of their droplet size could be due to droplet coalescence.

### *Droplet morphology*

Optical images of oil droplets were analyzed as fresh ( $t=0$ ) and after 96 h of storage to evaluate the possible destabilization mechanisms of emulsions (Fig. 3). The oil droplet size of all emulsions observed under optical microscopy is highly compatible to their DSD determined by static light scattering method (Fig. 2).

For the fresh emulsions ( $t=0$ ), droplet flocculation was witnessed for la-eGGM, la-sGGM, ha-sGGM and sGX emulsions while individual droplets were observed in the other hemicellulose-stabilized samples. This suggests that characteristics and composition of hemicellulose stabilizers affect emulsion breakdown. Removing acetyl groups and/or preserving the native lignin from hemicellulose structure promote flocculation of emulsions. Visual observation from the optical images reveals that hemicellulose-stabilized emulsions (ha-sGGM, la-sGGM, ha-eGGM, la-eGGM, CMGGM, eGX, sGX and CMGX) contained many oil droplets with a diameter of several micrometres. However, a lower extent of droplet flocculation and fewer large oil droplets were seen for CMGGM and CMGX emulsions, indicating that increasing surface charge of hemicellulose stabilizers inhibits their emulsion droplet aggregation and flocculation. Meanwhile, MC and CMC emulsions were mainly composed of small and separated oil droplets ( $< 100 \text{ nm}$ ). aCNC and nCNC emulsions exhibited the droplet aggregation with higher compacted degree than that observed for hemicellulose-stabilized samples. These aggregates seem to be intact under stirring during sample dispersion for droplet size measurement via static light scattering method (e.g. Mastersizer measurement), resulting in a large oil droplet diameter. Another possible reason for oil droplet aggregation of aCNC and nCNC emulsions is due to their high viscosity which prevents the droplet dispersion on the slide during optical microscopic analyses.

After storage for 96 h, flocculated and larger droplets (which are caused by coalescence) were apparent in all GGM-, GX- and CNC-stabilized emulsions while oil droplets in MC and CMC were evenly separated and remained as individual entities, indicating high stability of these emulsions.

### Turbiscan

Physical stability of emulsions over 96 h of storage indicated TSI is illustrated in Fig. 4, and fitting parameters ( $TSI_{max}$  and  $K$ ) are reported in Table S2 (Supplementary materials). Higher TSI values indicate lower stability of the emulsions. For hemicellulose-stabilized emulsions, the lowest stability was observed for la-eGGM and la-sGGM. Comparing these emulsions to ha-eGGM and ha-sGGM emulsions suggests that the removal of acetyl groups from the GGM structure resulted in a reduction of its capacity to stabilize emulsions. Due to lipophilic properties of acetyl groups, deacetylation of GGM alters its overall polarity, making it less lipophilic, and therefore having a lower emulsifying capacity (Lehtonen et al. 2018; Li et al. 2020). For both GGM and GX, at similar degrees of acetylation, emulsions prepared from spray-dried samples (la-sGGM, ha-sGGM and sGX) were more stable than those produced from ethanol-precipitated counterparts (la-eGGM, ha-eGGM and eGX). This indicated that the lignin residues in sGGM and sGX play an important

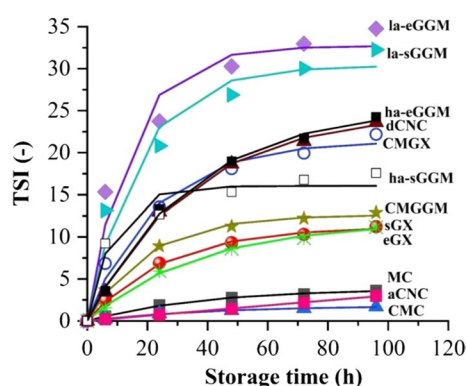


**Fig. 4** Global Turbiscan stability index (TSI) as a function of time during storage at 22 °C of emulsions prepared from different stabilizers. Please refer to Table 1 for the sample codes. For each sample, the marker symbols represent average experimental TSI data while the solid line shows the fitting with a 95% confidence interval obtained from Eq. (3)

role in stabilization of the oil droplets against creaming. These results are well aligned with recently reported findings about the emulsifying-enhanced roles of residual lignins in GGM and GX (Carvalho et al. 2021). The study suggested that preserving the lignin in GGM and GX promoted their anchoring to the droplet interface, and thereby their emulsion stabilization capacity.

As illustrated in Fig. 4, in the native structure, GX had a higher emulsion stabilization capacity than GGM. These can be explained by a combination of several reasons such as their composition, and molecular structure and molar mass. Unlike GGM, GX is also rich in linear-structure glucomannan, i.e. 7.6% in eGX and 6.3% in sGX (Carvalho et al. 2021), and these polysaccharides with a less branched structure were reported to enhance the long-term stability of emulsions by covering the droplet surface more efficiently (Alba et al. 2021). Other different characteristics between GX and GGM are acetyl content, degree of acetylation and absolute  $\zeta$ -potential, with higher values being reported for the former (Table 1), and as aforementioned, the hemicelluloses with the higher values of acetyl content, degree of acetylation and absolute  $\zeta$ -potential had the better emulsifying capacity. A higher emulsion stabilization capacity of GX than GGM was also reported (Carvalho et al. 2021).

As expected, the introduction of negatively charged carboxymethylated groups into GGM markedly increased its emulsion stability (CMGGM). However, an opposite result was observed for GX in which its carboxymethylation (CMGX) significantly reduced its emulsifying capacity, to a level even considerably lower than CMGGM despite their higher absolute  $\zeta$ -potential values (Fig. 1). This confirmed that surface charge alone did not define the emulsifying capacity of hemicelluloses. One possible explanation could be the degree of substitution of carboxymethyl groups (e.g., 0.33 in CMGX and 0.46 in CMGGM), which might affect the hydrophilic-lipophilic balance of carboxymethylated hemicelluloses, and thereby their emulsifying capacity. However, this assumption needs further investigation.

As detailed in Fig. 4, over 96 h of storage, CMC, MC and aCNC emulsions had the lowest TSI values, indicating that their capacity to stabilize emulsions was higher than that of all forms of investigated hemicellulose stabilizers. High stability of CMC and aCNC emulsions could be explained by the

**Table 3** Viscosity measured at shear rate of 100 1/s of citric buffer, hexadecane, continuous phases containing 1% (w/w) stabilizers, and corresponding emulsions as fresh (t=0) and after 96 h of storage. Please refer to Table 1 for the sample codes

Samples	Viscosity (mPa.s)			
	Continuous phases		Emulsions	
	t=0	96 h	t=0	96 h
Citric buffer	0.95 ± 0.03			
Hexadecane	3.33 ± 0.01			
la-eGGM	1.16 ± 0.01 <sup>a</sup>	1.17 ± 0.05 <sup>a</sup>	1.85 ± 0.16 <sup>ab</sup>	1.97 ± 0.01 <sup>ab</sup>
la-sGGM	1.18 ± 0.03 <sup>a</sup>	1.09 ± 0.00 <sup>a</sup>	2.28 ± 0.66 <sup>ab</sup>	1.80 ± 0.34 <sup>ab</sup>
ha-eGGM	1.09 ± 0.02 <sup>a</sup>	1.14 ± 0.03 <sup>a</sup>	1.38 ± 0.02 <sup>ab</sup>	1.35 ± 0.00 <sup>ab</sup>
ha-sGGM	1.03 ± 0.03 <sup>a</sup>	1.11 ± 0.00 <sup>a</sup>	1.47 ± 0.04 <sup>ab</sup>	1.72 ± 0.35 <sup>ab</sup>
CMGGM	1.19 ± 0.07 <sup>a</sup>	1.09 ± 0.02 <sup>a</sup>	1.32 ± 0.00 <sup>ab</sup>	1.35 ± 0.04 <sup>ab</sup>
eGX	1.11 ± 0.05 <sup>a</sup>	1.15 ± 0.05 <sup>a</sup>	1.32 ± 0.12 <sup>ab</sup>	1.29 ± 0.09 <sup>ab</sup>
sGX	1.11 ± 0.01 <sup>a</sup>	1.05 ± 0.01 <sup>a</sup>	1.35 ± 0.03 <sup>ab</sup>	1.29 ± 0.07 <sup>ab</sup>
CMGX	1.01 ± 0.04 <sup>a</sup>	1.09 ± 0.05 <sup>a</sup>	1.34 ± 0.01 <sup>ab</sup>	1.37 ± 0.08 <sup>ab</sup>
MC	4.35 ± 0.13 <sup>b</sup>	4.47 ± 0.57 <sup>b</sup>	3.88 ± 0.49 <sup>b</sup>	3.66 ± 0.19 <sup>ab</sup>
CMC	7.03 ± 0.45 <sup>c</sup>	6.62 ± 0.28 <sup>c</sup>	7.83 ± 0.87 <sup>c</sup>	7.51 ± 0.43 <sup>ab</sup>
aCNC	35.28 ± 3.94 <sup>e</sup>	38.52 ± 0.40 <sup>e</sup>	24.24 ± 5.36 <sup>e</sup>	25.76 ± 4.73 <sup>ab</sup>
dCNC	10.64 ± 2.5 <sup>d</sup>	11.68 ± 0.31 <sup>d</sup>	10.71 ± 0.64 <sup>d</sup>	11.98 ± 0.36 <sup>ab</sup>

A one-way analysis of variance (ANOVA) and Tukey test were used as a post-hoc test for a pairwise comparison of the means with a statistically significant difference at  $p \leq 0.05$  using OriginPro 2020 (OriginLab Corporation, Northampton, MA, USA). Within the same column, means with different letters indicated statistically significant differences among samples

combination of their high surface charge (Fig. 1) and high viscosity (Table 3) while the storage stability of MC emulsions is possibly associated with small oil droplet diameter (Table S1). Lower stability of dCNC emulsions, as compared to aCNC ones, is possibly attributed to its larger droplet size (Table S1) and lower surface charge (Fig. 1).

### Rheological properties

As discussed in previous sections,  $\zeta$ -potential, size of oil droplets, and characteristics and composition of stabilizers can partly explain the stability of emulsions investigated in this study. Therefore, it is worthy to evaluate other factors such as rheological properties of continuous phases and emulsions to further explain the capacity and/or mechanisms of stabilizers to produce stable emulsions. Flow behavior of emulsions depends on many parameters, especially inter-droplet forces which are determined by stabilizers; therefore its measurement provides information about the arrangement of oil droplets. In this study, due to the low viscosity of the hemicellulose-based samples, repeatable results of flow measurements

were only obtained at shear rates above 10 1/s. The results of continuous phases (Figure S4) and emulsions (Fig. 5) within the shear rate range of 10–1000 1/s are presented with increasing (I) and decreasing (D) shear rate. Oscillatory data is shown only for samples where repeatable results were obtained, that is, for MC, CMC, aCNC and dCNC (Figures S5 and S6). The viscosities at shear rate of 100 1/s of citric buffer, hexadecane, continuous phases and emulsions as freshly prepared (t=0) and after 96 h of storage are summarized in Table 3. For fresh continuous phases (Figure S4), all GGM and GX samples showed Newtonian behavior. The Newtonian behavior of PHWE GGM solutions at concentrations up to 30% has also been reported earlier (Bhattarai et al. 2020a, b; Mikkonen et al. 2016a). However, solutions of GGM extracted by TMP were reported to have a higher viscosity and show shear-thinning behavior at concentrations above 0.5% (Xu et al. 2009). This rheological behavior of TMP GGM is possibly associated with its higher molar mass (48,000 g/mol), which is much higher than that of PHWE GGM in this study (i.e. 2800–13,000 g/mol). Newtonian behavior was also observed for citric buffer, hexadecane oil, MC



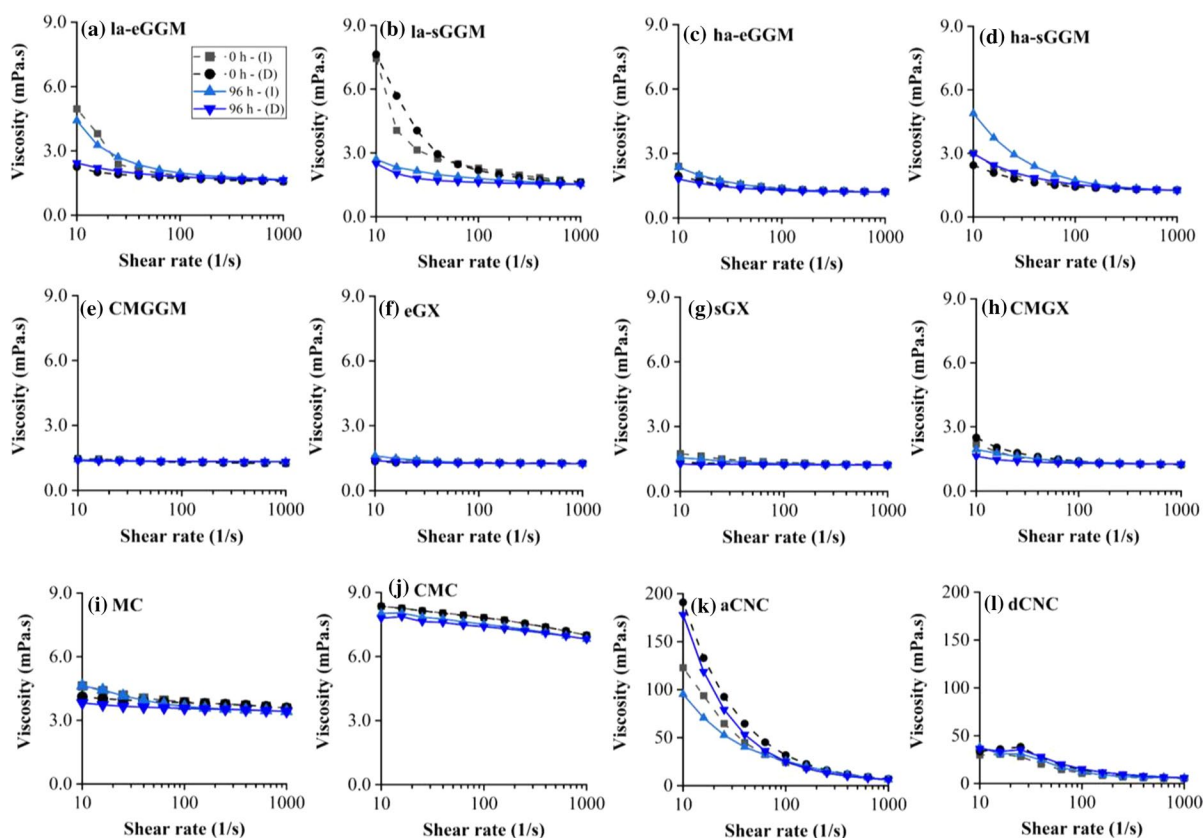


**Fig. 5** Flow curves of emulsions prepared from different stabilizers measured at shear rates of 10–1000 1/s, which are freshly prepared (0 h) and after 96 h of storage. Two cycles of

shearing included (I): increasing of shear rate from 10 to 1000 1/s, and (D): decreasing of shear rate from 1000 to 10 1/s. Please refer to Table 1 for the sample codes

and CMC samples while aCNC and dCNC samples displayed shear-thinning behavior. The rheological behavior of all continuous phases were the same after 96 h of storage (Figure S4).

Regarding emulsions, there was a clear difference in flow behaviors among hemicellulose-stabilized emulsions. Fresh ha-sGGM, la-sGGM, ha-eGGM, la-eGGM, and CMGX emulsions were shear-thinning. Meanwhile, CMGGM, sGX and eGX emulsions behaved like their continuous phases and showed Newtonian flow behavior. These results suggested the surface charge of hemicelluloses rather than lignin content affects flow behavior of emulsions made from them. Also, removal of acetyl groups from GGM structure did not affect the flow behavior of GGM-stabilized emulsions. Despite similarity in viscosity at 100 1/s between CMGX and CMGGM emulsions (Table 3), differences in their flow behavior could partially explain their emulsion stability differences

(Fig. 4). All fresh cellulose-stabilized emulsions (e.g., MC, CMC, aCNC and dCNC) exhibited pronounced shear-thinning behavior with a much higher degree being observed for Pickering stabilizers. These results are in agreement with previous findings for cellulose-stabilized emulsions despite the differences in oil phase and concentration (Arancibia et al. 2013; Miao et al. 2021; Zhang et al. 2017).

As indicated in Fig. 5, the flow behavior of hemicellulose-stabilized emulsions, especially GGM ones, were similar to those of Pickering emulsions (aCNC and dCNC), rather than soluble cellulose-stabilized emulsions (MC and CMC). This suggests that hemicelluloses possibly stabilize emulsions by an adsorbed layer of insoluble particles. As reported, GGM and GX obtained by PHWE are a complex mixture of different compounds consisting of hemicelluloses and residual lignin (Lehtonen et al. 2018). Lignin is insoluble and forms particles at neutral pH

(Evstigneev 2010; Sewring et al. 2019). Also, during spray drying of hemicelluloses, insoluble lignin particles with a size of a few micrometres could be formed (Miao and Hamad 2017). The adsorption of the insoluble lignin particles on droplet interface of hemicellulose-stabilized emulsions makes their flow behavior more like the Pickering emulsions. In previous work by Mikkonen et al. (2016a) on rheological properties of hemicellulose-stabilized emulsions (e.g., PHWE GGM and GX) at higher hemicellulose and oil phase concentrations it was reported that the steric repulsion was assisted by the adsorption of particulate GGM and GX aggregates. These act as Pickering stabilizers and it was the principle emulsion stabilization mechanism of GGM and GX.

Figure 5 shows hysteresis loops between the up- and down-shearing curves, where differences represent the energy associated with the structural changes of the samples after shearing. Hysteresis were observed for all fresh studied emulsions, except CMC and CMGGM ones. The hysteresis phenomenon in these samples was more profound after 96 h of storage, which could be because of the appearance of larger droplet size resulting from coalescence and creaming.

In a study by Bhattarai et al. (2020a, b) for PHWE GGM, the authors reported that at pH 4.6, similar to the pH used in this study, GGM solution formed aggregates with size of several hundreds of micrometres after 48 h of storage at room temperature (~22 °C). These aggregates, after dissociation by high-intensity mechanical shearing, were able to re-associate during storage. Combined effects of the aggregation of hemicelluloses themselves and presence of oil droplets alter the rheological behavior of their emulsions as compared to their corresponding continuous phase. The observed hysteresis could result from the structural breakdown of the aggregates and/or formation of a new structure from broken aggregates under shearing. The differences in rheological behavior including the shear thinning and hysteresis of la-sGGM and la-eGGM emulsions compared with other hemicellulose-stabilized emulsions could be explained by low DA in the former. Differences in the flow curves at low shear rate between GGM- and GX-stabilized emulsions possibly indicate their differences in emulsifying capacity. Due to their differences in structure and composition, they might experience the aggregation differently.

The agglomeration of polysaccharides, including wood hemicelluloses in an aqueous environment was also reported elsewhere (Kishani et al. 2019, 2018; Parikka et al. 2010).

To monitor the changes in viscosity under constant shear, the samples were kept at shear rate of 10 and 100, 1/s for 20 min (Fig. 6). MC, CMC and CMGGM displayed constant viscosity at both shear rates over the tested time range, suggesting the microstructures of emulsions did not change under these conditions. Other emulsion samples exhibited viscosity changes over time, especially at a shear rate of 10 (1/s), ascribing to the structural reorganization of emulsions under shearing. This behavior can be explained by the presence of insoluble particles on the oil droplet surface and in water phase of emulsions, and their interactions under low shear rate results in an increase of the emulsion viscosity. However, under high shear rate (100, 1/s), their interactions were destroyed, leading to constant viscosity. Similar rheological behaviors of CNC emulsions at various CNC concentrations (0.6, 1.2 and 2.4%) and shear rates (0.1, 1.0 and 10, 1/s) have been reported (Miao et al. 2021). The viscosity vs. time responses under a constant shear rate of hemicellulose-stabilized emulsions, except CMGGM and la-sGGM ones, were similar to Pickering emulsions stabilized by aCNC and nCNC, suggesting their similarity in droplet adsorption behaviors during emulsification. The differences in flow behaviors under constant shearing of CMGGM and la-sGGM emulsions to other hemicellulose-stabilized ones are probably due to high solubility of CMGGM ascribed by carboxymethylation (Gabriel et al. 2020), which make it's behavior like that of soluble celluloses (MC, and CMC); and low solubility of la-sGGM resulted by deacetylation and presence of insoluble lignin, as mentioned above.

As shown in Table 3, for continuous phases, all fresh GGM and GX stabilizers had similar viscosities (e.g., 1.01–1.19 mPa.s), and was much lower than that of fresh cellulose stabilizers (e.g., MC, CMC, aCNC and dCNC). After 96 h of storage, viscosity of all investigated continuous phases were almost unchanged. Similar viscosity levels were also observed for emulsions. The higher viscosity of cellulose-stabilized emulsions than hemicellulose-stabilized counterparts enables the reduction of the mobility and probability for collision of droplets; decreasing flocculation and coalescence, and

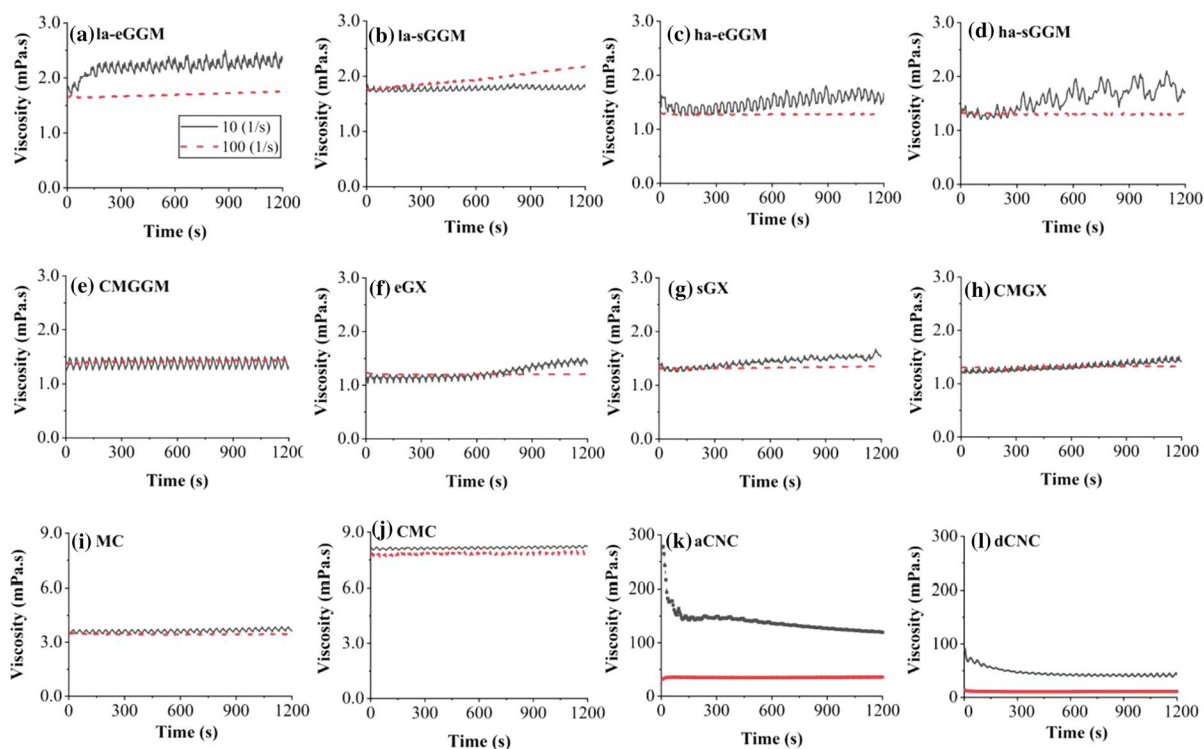


**Fig. 6** Flow curves of fresh emulsions prepared from different stabilizers under shear rates of 10 and 100 1/s over a period of 20 min. Please refer to Table 1 for the sample codes

reducing the creaming rate, and therefore improving emulsion stability (Dickinson 2009). Similar viscosity obtained for all GGM- and GX-stabilized emulsions indicates that the differences in characteristics and composition of the hemicelluloses did not cause any differences in viscosity, and that the differences in their emulsion stability could not be explained by viscosity alone.

## Conclusion

Wood hemicelluloses recovered by PHWE method from spruce (GGM) and birch (GX) are good emulsion stabilizers of which GX produces emulsions with smaller droplets than GGM. This is possibly due to a higher charged surface and higher degree of acetylation of GX. The composition and properties of hemicelluloses greatly affected the stability and other properties of emulsions produced from them. For GGM, although preserving the native lignin and acetyl structure did not have a major effects on surface

charge, it helped to generate small emulsion droplets, thereby improving their emulsifying properties. Similar effects of preserving the native lignin on surface charge and emulsion stability were also witnessed for GX. Carboxymethylation to introduce anionic groups to hemicelluloses showed opposite effects on their emulsifying ability between GGM and GX in which the enhancement was found only for GGM. Regardless of the composition and properties of GGM and GX, the continuous phases and emulsions had very low viscosity, indicating that viscosity does not play any role in emulsion stabilization. By comparing flow behaviors of GGM and GX emulsions to those of established cellulose-stabilized emulsions, it is evident that the presence of insoluble particles that possibly function as Pickering stabilizers are found in GGM- and GX-stabilized emulsions. These results confirm the emulsion stabilization mechanisms from the viewpoint of rheological properties of emulsions. Unlike celluloses, hemicelluloses can stabilize emulsions without increasing their viscosity, even when a high concentration of hemicelluloses is employed.

This makes emulsion preparation from hemicelluloses easier and less energy-consuming than from celluloses. Low viscosity emulsions are required for many applications in foods, cosmetics, personal care products and paints. These findings provide a comprehensive understanding about the effects of properties and types of wood hemicelluloses on their ability to stabilize emulsions. This will allow the selection of a suitable hemicellulose for a specific application, and guide the hemicellulose recovery processes to control desirable properties.

**Acknowledgments** The authors acknowledge the Academy of Finland (project no. 322514) for funding, and Mr. Troy Faithfull for his proofreading. The use of NMR facilities at the Danish Center for Ultrahigh-Field NMR Spectroscopy funded by the Danish Ministry of Higher Education and Science (AU-2010-612-181) is acknowledged.

**Author contributions** TMH: Conceptualization, Methodology, Investigation, Formal Analysis, Visualization, Data Curation, Writing—Original Draft, Writing—Review & Editing. FA: Conceptualization, Methodology, Investigation, Formal Analysis, Visualization, Data curation, Writing—Original Draft, Writing—Review & Editing. SH: Methodology, Resources, Formal Analysis, Writing—Review & Editing. EIF: Methodology, Resources, Formal Analysis, Writing—Review & Editing. DWJ: Methodology, Resources, Formal Analysis, Writing—Review & Editing. TV: Methodology, Resources, Formal Analysis, Writing—Review & Editing. KSM: Conceptualization, Methodology, Supervision, Investigation, Data Curation, Visualization, Project Administration, Funding Acquisition, Writing—Review & Editing.

**Funding** Open Access funding provided by University of Helsinki including Helsinki University Central Hospital. This work was supported by the Academy of Finland (project no. 322514).

## Declarations

**Conflict of interest** All authors certify that they have no affiliations with or involvement in any organization or entity with any financial interest or non-financial interest in the subject matter or materials discussed in this manuscript.

**Open Access** This article is licensed under a Creative Commons Attribution 4.0 International License, which permits use, sharing, adaptation, distribution and reproduction in any medium or format, as long as you give appropriate credit to the original author(s) and the source, provide a link to the Creative Commons licence, and indicate if changes were made. The images or other third party material in this article are included in the article's Creative Commons licence, unless indicated otherwise in a credit line to the material. If material is not included in the article's Creative Commons licence and your intended use is not permitted by statutory regulation or exceeds the permitted use, you will need to obtain permission directly from the copyright holder. To view a copy of this licence, visit <http://creativecommons.org/licenses/by/4.0/>.

## References

- Alba K, Dimopoulou M, Kontogiorgos V (2021) Baobab polysaccharides as emulsifiers. *LWT* 144:111235. <https://doi.org/10.1016/j.lwt.2021.111235>
- Al-Rudainy B, Galbe M, Schagerlöf H, Wallberg O (2018) Antisolvent precipitation of hemicelluloses, lignosulfonates and their complexes from ultrafiltrated spent sulfite liquor (SSL). *Holzforschung* 72:839–850. <https://doi.org/10.1515/hf-2017-0218>
- Andersson A, Persson T, Zacchi G, Ståhlbrand H, Jönsson A-S (2007) Comparison of diafiltration and size-exclusion chromatography to recover hemicelluloses from process water from thermomechanical pulping of spruce. *Appl Biochem Biotechnol* 137:971–983. <https://doi.org/10.1007/s12010-007-9112-9>
- Arancibia C, Bayarri S, Costell E (2013) Comparing carboxymethyl cellulose and starch as thickeners in oil/water emulsions. Implications on rheological and structural properties. *Food Biophys* 8:122–136. <https://doi.org/10.1007/s11483-013-9287-2>
- Bai L, Lv S, Xiang W, Huan S, McClements DJ, Rojas O (2019) Oil-in-water Pickering emulsions via microfluidization with cellulose nanocrystals: 1. Formation and stability. *Food Hydrocoll* 96:699–708. <https://doi.org/10.1016/j.foodhyd.2019.04.038>
- Bhattacharjee S (2016) DLS and zeta potential—what they are and what they are not? *JCR* 235:337–351. <https://doi.org/10.1016/j.jconrel.2016.06.017>
- Bhattarai M, Pitkänen L, Kitunen V, Korpinen R, Ilvesniemi H, Kilpeläinen PO, Lehtonen M, Mikkonen KS (2019) Functionality of spruce galactoglucomannans in oil-in-water emulsions. *Food Hydrocoll* 86:154–161. <https://doi.org/10.1016/j.foodhyd.2018.03.020>
- Bhattarai M, Valoppi F, Hirvonen S-P, Hietala S, Kilpeläinen P, Aseyev V, Mikkonen KS (2020a) Time-dependent self-association of spruce galactoglucomannans depends on pH and mechanical shearing. *Food Hydrocoll* 102:105607. <https://doi.org/10.1016/j.foodhyd.2019.105607>
- Bhattarai M, Sulaeva I, Pitkänen L, Kontro I, Tenkanen M, Potthast A, Mikkonen KS (2020b) Colloidal features of softwood galactoglucomannans-rich extract. *Carbohydr Polym* 241:116368. <https://doi.org/10.1016/j.carbpol.2020.116368>
- Candido RG, Gonçalves AR (2016) Synthesis of cellulose acetate and carboxymethylcellulose from sugarcane straw. *Carbohydr Polym* 152:679–686. <https://doi.org/10.1016/j.carbpol.2016.07.071>
- Carvalho DMD, Lahtinen MH, Lawoko M, Mikkonen KS (2020) Enrichment and identification of lignin-carbohydrate complexes in softwood extract. *ACS Sustain Chem Eng* 8(31):11795–11804. <https://doi.org/10.1021/acssuschemeng.0c03988>
- Carvalho DM, Lahtinen M, Bhattarai M, Lawoko M, Mikkonen KS (2021) Active role of lignin in anchoring wood-based stabilizers to the emulsion interface. *Green Chem* 23:9084–9098. <https://doi.org/10.1039/D1GC02891J>
- Chadni M, Grimi N, Bals O, Ziegler-Devin I, Brosse N (2019a) Steam explosion process for the selective extraction of

- hemicelluloses polymers from spruce sawdust. *Ind Crops Prod* 141:111757. <https://doi.org/10.1016/j.indcrop.2019.111757>
- Chadni M, Grimi N, Ziegler-Devin I, Brosse N, Bals O (2019b) High voltage electric discharges treatment for high molecular weight hemicelluloses extraction from spruce. *Carbohydr Polym* 222:115019. <https://doi.org/10.1016/j.carbpol.2019.115019>
- Chong S-L, Koutaniemi S, Virkki L, Pynnönen H, Tuomainen P, Tenkanen M (2013) Quantitation of 4-O-methylglucuronic acid from plant cell walls. *Carbohydr Polym* 91:626–630. <https://doi.org/10.1016/j.carbpol.2012.08.078>
- Costa C, Medronho B, Lindman B, Edlund H, Norgren M (2021) Cellulose as a natural emulsifier: from nanocelluloses to macromolecules. In: Sand A, Banga S (eds) *Cellulose science and derivatives*. IntechOpen, London
- Dickinson E (2009) Hydrocolloids as emulsifiers and emulsion stabilizers. *Food Hydrocoll* 23:1473–1482. <https://doi.org/10.1016/j.foodhyd.2008.08.005>
- Evtstigneev E (2010) Specific features of lignin dissolution in aqueous and aqueous-organic media. *Russ J Appl Chem* 83:509–513. <https://doi.org/10.1134/S1070427210030250>
- Gabriel L, Tied A, Heinze T (2020) Carboxymethylation of polysaccharides—A comparative study. *Cellulose Chem Technol* 54:835–844
- Giummarella N, Lawoko M (2017) Structural insights on recalcitrance during hydrothermal hemicellulose extraction from wood. *CS Sustain Chem Eng* 5:5156–5165. <https://doi.org/10.1021/acssuschemeng.7b00511>
- Gröndahl M, Telemann A, Gatenholm P (2003) Effect of acetylation on the material properties of glucuronoxylan from aspen wood. *Carbohydr Polym* 52:359–366. [https://doi.org/10.1016/S0144-8617\(03\)00014-6](https://doi.org/10.1016/S0144-8617(03)00014-6)
- Hannuksela T, Holmbom B (2004) Stabilization of wood-resin emulsions by dissolved galactoglucomannans and galactomannans. *J Pulp Paper Sci* 30:159–164
- Heinze T, El Seoud OA, Koschella A (2018) *Cellulose derivatives: synthesis, structure, and properties*. Springer, Berlin
- Hromádková Z, Ebringerová A, Malovíková A (2005) The structural, molecular and functional properties of lignin-containing beechwood glucuronoxylan. *Macromol Symp* 232:19–26. <https://doi.org/10.1002/masy.200551403>
- Jääskeläinen AS, Saariaho AM, Vuorinen T (2005) Quantification of lignin and hexenuronic acid in bleached hardwood kraft pulps: a new calibration method for UVRR spectroscopy and evaluation of the conventional methods. *J Wood Chem Technol* 25:51–65. <https://doi.org/10.1081/WCT-200058239>
- Johnson RL, Schmidt-Rohr K (2014) Quantitative solid-state <sup>13</sup>C NMR with signal enhancement by multiple cross polarization. *J Magn Reson* 239:44–49. <https://doi.org/10.1016/j.jmr.2013.11.009>
- Juha AV, Tao S, Susanna K, Ville A (2012) Model for degradation of galactoglucomannan in hot water extraction conditions. *Ind Eng Chem Res* 51(31):10338–10344. <https://doi.org/10.1021/ie3000826>
- Kilpeläinen P, Hautala S, Byman O, Tanner L, Korpinen R, Lillandt MK, Pranovich A, Kitunen V, Willför S, Ilvesniemi HS (2014) Pressurized hot water flow-through extraction system scale up from the laboratory to the pilot scale. *Green Chem* 16:3186–3194. <https://doi.org/10.1039/C4GC00274A>
- Kishani S, Vilaplana F, Xu W, Xu C, Wågberg L (2018) Solubility of softwood hemicelluloses. *Biomacromol* 19:1245–1255. <https://doi.org/10.1021/acs.biomac.8b00088>
- Kishani S, Escalante A, Toriz G, Vilaplana F, Gatenholm P, Hansson P, Wågberg L (2019) Experimental and theoretical evaluation of the solubility/insolubility of spruce xylan (*Arabino glucuronoxylan*). *Biomacromolecules* 20:1263–1270. <https://doi.org/10.1021/acs.biomac.8b01686>
- Klemm D, Heublein B, Fink HP, Bohn A (2005) Cellulose: fascinating biopolymer and sustainable raw material. *Angew Chem Int Ed* 44:3358–3393. <https://doi.org/10.1002/anie.200460587>
- Kynkäänniemi E, Lahtinen MH, Jian C, Salonen A, Hatanpää T, Mikkonen KS, Pajari AM (2022) Gut microbiota can utilize prebiotic birch glucuronoxylan in production of short-chain fatty acids in rats. *Food Funct* 13:3746–3759. <https://doi.org/10.1039/D1FO03922A>
- Lahtinen MH, Valoppi F, Juntti V, Heikkinen S, Kilpeläinen PO, Maina NH, Mikkonen KS (2019) Lignin-rich PHWE hemicellulose extracts responsible for extended emulsion stabilization. *Front Chem* 7:871. <https://doi.org/10.3389/fchem.2019.0087>
- Laine C, Tamminen T, Vikkula A, Vuorinen T (2002) Methylation analysis as a tool for structural analysis of wood polysaccharides. *Holzforchung* 56:607–614. <https://doi.org/10.1515/HF.2002.093>
- Lehtonen M, Merinen M, Kilpeläinen PO, Xu C, Willför SM, Mikkonen KS (2018) Phenolic residues in spruce galactoglucomannans improve stabilization of oil-in-water emulsions. *J Colloid Interface Sci* 512:536–547. <https://doi.org/10.1016/j.jcis.2017.10.097>
- Li Y-F, Yue P-P, Hao X, Bian J, Ren J-L, Peng F, Sun R-C (2020) Comparison of emulsifying capacity of two hemicelluloses from moso bamboo in soy oil-in-water emulsions. *RSC Adv* 10:4657–4663. <https://doi.org/10.1039/C9RA08636F>
- Lundqvist J, Jacobs A, Palm M, Zacchi G, Dahlman O, Stålbbrand H (2003) Characterization of galactoglucomannan extracted from spruce (*Picea abies*) by heat-fractionation at different conditions. *Carbohydr Polym* 51:203–211. [https://doi.org/10.1016/S0144-8617\(02\)00111-X](https://doi.org/10.1016/S0144-8617(02)00111-X)
- McClements DJ (2005) *Food emulsions: principles, practices, and techniques*, 2nd edn. CRC Press, New York
- Melro E, Alves L, Antunes FE, Medronho B (2018) A brief overview on lignin dissolution. *J Mol Liq* 265:578–584. <https://doi.org/10.1016/j.molliq.2018.06.021>
- Miao C, Hamad WY (2017) Controlling lignin particle size for polymer blend applications. *J Appl Polym Sci* 134:44669. <https://doi.org/10.1002/app.44669>
- Miao C, Mirvakili M-N, Hamad WY (2021) A rheological investigation of oil-in-water Pickering emulsions stabilized by cellulose nanocrystals. *J Colloid Interface Sci* 608(3):2820–2829. <https://doi.org/10.1016/j.jcis.2021.11.010>
- Mikkonen KS (2020) Strategies for structuring diverse emulsion systems by using wood lignocellulose-derived stabilizers. *Green Chem* 22:1019–1037. <https://doi.org/10.1039/C9GC04457D>

- Mikkonen KS, Tenkanen M, Cooke P, Xu C, Rita H, Willför S, Holmbom B, Hicks KB, Yadav MP (2009) Mannans as stabilizers of oil-in-water beverage emulsions. *LWT* 42:849–855. <https://doi.org/10.1016/j.lwt.2008.11.010>
- Mikkonen KS, Merger D, Kilpeläinen P, Murtomäki L, Schmidt US, Wilhelm MJ (2016a) Determination of physical emulsion stabilization mechanisms of wood hemicelluloses via rheological and interfacial characterization. *Soft Matter* 12:8690–8700. <https://doi.org/10.1039/C6SM01557C>
- Mikkonen KS, Xu C, Berton-Carabin C, Schroën KJ (2016b) Spruce galactoglucomannans in rapeseed oil-in-water emulsions: Efficient stabilization performance and structural partitioning. *Food Hydrocoll* 52:615–624. <https://doi.org/10.1016/j.foodhyd.2015.08.009>
- Mikkonen KS, Kirjoranta S, Xu C, Hemming J, Pranovich A, Bhattarai M, Peltonen L, Kilpeläinen P, Maina N, Tenkanen M, Lehtonen M, Willför S (2019) Environmentally-compatible alkyd paints stabilized by wood hemicelluloses. *Ind Crops Prod* 133:212–220. <https://doi.org/10.1016/j.indcrop.2019.03.017>
- O'sullivan J, Murray B, Flynn C, Norton I (2015) Comparison of batch and continuous ultrasonic emulsification processes. *J Food Eng* 167:114–121. <https://doi.org/10.1016/j.jfoodeng.2015.05.001>
- Pandey A, Derakhshandeh M, Kedzior SA, Pilapil B, Shomrat N, Segal-Peretz T, Bryant SL, Trifkovic MJ (2018) Role of interparticle interactions on microstructural and rheological properties of cellulose nanocrystal stabilized emulsions. *J Colloid Interface Sci* 532:808–818. <https://doi.org/10.1016/j.jcis.2018.08.044>
- Parikka K, Leppänen A-S, Pitkanen L, Reunanen M, Willför S, Tenkanen M (2010) Oxidation of polysaccharides by galactose oxidase. *J Agric Food Chem* 58:262–271. <https://doi.org/10.1021/jf902930t>
- Petzold K, Schwikal K, Heinze T (2006) Carboxymethyl xylan—synthesis and detailed structure characterization. *Carbohydr Polym* 64:292–298. <https://doi.org/10.1016/j.carbpol.2005.11.037>
- Schönberg C, Oksanen T, Suurnäkki A, Kettunen H, Buchert J (2001) The importance of xylan for the strength properties of spruce kraft pulp fibres. *Holzforschung* 55:639–644. <https://doi.org/10.1515/HF.2001.104>
- Sewring T, Durruty J, Schneider L, Schneider H, Mattsson T, Theliander H (2019) Acid precipitation of kraft lignin from aqueous solutions: the influence of pH, temperature, and xylan. *J Wood Chem Technol* 39:1–13. <https://doi.org/10.1080/02773813.2018.1488870>
- Sixta H (2006) *Handbook of pulp*. Wiley-VCH Verlag GmbH & Co., Kga, Weinheim
- Sjöström E (1993) *Wood chemistry: fundamentals and applications*. Academic Press, San Diego
- Song T, Pranovich A, Summers I, Holmbom B (2008) Extraction of galactoglucomannan from spruce wood with pressurised hot water. *Holzforschung* 62:659–666. <https://doi.org/10.1515/HF.2008.131>
- Sundberg A, Sundberg K, Lilland C, Holmbom B (1996) Determination of hemicelluloses and pectins in wood and pulp fibres by acid methanolysis and gas chromatography. *Nord Pulp Pap Res J* 11:216–219. <https://doi.org/10.3183/npprj-1996-11-04-p216-219>
- Tadros TF (2016) *Emulsions: formation, stability, industrial applications*. Walter de Gruyter GmbH & Co KG, Berlin
- Teleman A, Harjunpää V, Tenkanen M, Buchert J, Hausalo T, Drakenberg T, Vuorinen T (1995) Characterisation of 4-deoxy- $\beta$ -l-threo-hex-4-enopyranosyluronic acid attached to xylan in pine kraft pulp and pulping liquor by  $^1\text{H}$  and  $^{13}\text{C}$  NMR spectroscopy. *Carbohydrate Res* 272:55–71. [https://doi.org/10.1016/0008-6215\(95\)96873-M](https://doi.org/10.1016/0008-6215(95)96873-M)
- Valoppi F, Lahtinen MH, Bhattarai M, Kirjoranta SJ, Juntti VK, Peltonen LJ, Kilpeläinen PO, Mikkonen KS (2019) Centrifugal fractionation of softwood extracts improves the biorefinery workflow and yields functional emulsifiers. *Green Chem* 21:4691–4705. <https://doi.org/10.1039/C9CG02007A>
- Wang L-X, Lee A-R, Yuan Y, Wang X-M, Lu T-J (2020) Preparation and FTIR, Raman and SEM characterizations of konjac glucomannan-KCl electrogels. *Food Chem* 331:127289. <https://doi.org/10.1016/j.foodchem.2020.127289>
- Waqar A, Susanna K, Andrey P, Ville A (2018) Physico-chemical modeling for pressurized hot water extraction of spruce wood. *Ind Eng Chem Res* 57(49):16664–16674. <https://doi.org/10.1021/acs.iecr.8b05097>
- Willför S, Sundberg K, Tenkanen M, Holmbom B (2008) Spruce-derived mannans—A potential raw material for hydrocolloids and novel advanced natural materials. *Carbohydr Polym* 72:197–210. <https://doi.org/10.1016/j.carbpol.2007.08.006>
- Xu C, Willför S, Holmlund P, Holmbom B (2009) Rheological properties of water-soluble spruce O-acetyl galactoglucomannans. *Carbohydr Polym* 75:498–504. <https://doi.org/10.1016/j.carbpol.2008.08.016>
- Xu C, Leppänen A-S, Eklund P, Holmlund P, Sjöholm R, Sundberg K, Willför S (2010) Acetylation and characterization of spruce (*Picea abies*) galactoglucomannans. *Carbohydr Res* 345:810–816. <https://doi.org/10.1016/j.carres.2010.01.007>
- Xu C, Eckerman C, Smeds A, Reunanen M, Eklund PC, Sjöholm R, Willför S (2011) Carboxymethylated spruce galactoglucomannans: preparation, characterisation, dispersion stability, water-in-oil emulsion stability, and sorption on cellulose surface. *Nord Pulp Pap Res J* 26:167–179. <https://doi.org/10.3183/npprj-2011-26-02-p167-178>
- Zeng Y, Yarbrough JM, Mittal A, Tucker MP, Vinzant TB, Decker SR, Himmel ME (2016) In situ label-free imaging of hemicellulose in plant cell walls using stimulated Raman scattering microscopy. *Biotechnol Biofuels* 9:256. <https://doi.org/10.1186/s13068-016-0669-9>
- Zhang M, Yang B, Liu W, Li S (2017) Influence of hydroxypropyl methylcellulose, methylcellulose, gelatin, poloxamer 407 and poloxamer 188 on the formation and stability of soybean oil-in-water emulsions. *Asian J Pharm Sci* 12:521–531. <https://doi.org/10.1016/j.ajps.2017.05.009>

**Publisher's Note** Springer Nature remains neutral with regard to jurisdictional claims in published maps and institutional affiliations.